MARMARA UNIVERSITY
INSTITUTE FOR GRADUATE STUDIES
IN PURE AND APPLIED SCIENCES

RATIONAL DESIGN OF NEW MATERIALS FOR HIGH-EFFICIENCY SPINTRONICS

Kevser HANCIOĞLU

MASTER THESIS

Department of Physics

Thesis Supervisor

Associate Professor Caner DEĞER

ISTANBUL, 2025

MARMARA UNIVERSITY
INSTITUTE FOR GRADUATE STUDIES
IN PURE AND APPLIED SCIENCES

RATIONAL DESIGN OF NEW MATERIALS FOR HIGH-EFFICIENCY SPINTRONICS

Kevser HANCIOĞLU

(521221005)

MASTER THESIS

Department of Physics

Thesis Supervisor

Associate Professor Caner DEĞER

ISTANBUL, 2025

ACKNOWLEDGEMENTS

I would like to express my gratitude to my supervisor, Associate Professor Caner Değer, for his guidance and contributions throughout this thesis. I am also thankful to my laboratory colleagues for their support during this process.

However, my deepest gratitude goes to my family. Their unwavering support, love, and patience have been my greatest sources of strength throughout every stage of this journey. They have always been by my side, providing moral support and empowering me to continue. My thanks cannot be adequately expressed in words.

April, 2025 **Kevser HANCIOĞLU**

CONTENTS

ÖZET

YÜKSEK VERİMLİ SPİNTRONİK MALZEMELERİN RASYONEL DİZAYNI

Bu çalışma, Formamidinyum Kurşun Triiyodür ($FAPbI_3$) yapısında kurşun (Pb) atomlarının geçiş metalleri ve nadir toprak elementleriyle değiştirilmesiyle yapısal, elektronik ve manyetik özelliklerin incelenmesini amaçlamaktadır. Çalışma kapsamında, yakın komşu (NN), üçüncü yakın komşu (TNN), bizmut katkılı TNN (Bi-TNN) ve platin katkılı TNN (Pt-TNN) etkileşimlerini içeren çeşitli konfigürasyonlar oluşturulmuştur.

Öncelikle, katkılanmış konfigürasyonlar için geometri optimizasyonları gerçekleştirilmiş, ardından tek nokta enerji hesaplamaları yapılmıştır. Daha sonra, sistemlerin manyetik davranışlarını incelemek amacıyla non-collinear (NCL) manyetik hesaplamalar uygulanmıştır. NCL hesaplamaları, bu çalışmanın temel amacı olan spintronik uygulamalara yönelik manyetik malzeme analizleri için kritik bir rol oynamıştır.

Tüm hesaplamalar Yoğunluk Fonksiyonel Teorisi (DFT) kullanılarak gerçekleştirilmiştir. Çalışma, formasyon enerjileri, exchange enerjileri, hacim değişimleri, yük yoğunluğu farkları (CDD) ve kısmi durum yoğunlukları (PDOS) gibi parametrelerin değerlendirilmesini içermektedir. Bu analizler, katkılanmış malzemelerin yapısal, elektronik ve manyetik özelliklerine dair ayrıntılı bir anlayış sağlamıştır. Ayrıca, katkı maddelerinin kafesin kararlılığı ve davranışı üzerindeki etkileri değerlendirilmiş ve elde edilen bulgular temel alınarak potansiyel uygulama alanları önerilmiştir.

ABSTRACT

RATIONAL DESIGN OF NEW MATERIALS FOR HIGH-EFFICIENCY SPINTRONICS

This study investigates the structural, electronic, and magnetic properties of Formamidinium Lead Triiodide ($FAPbI_3$) doped with selected transition metals and rare-earth elements, replacing lead (Pb) atoms in the lattice. Various configurations were created, including nearest-neighbor (NN), third-nearest-neighbor (TNN), bismuth-doped TNN (Bi-TNN), and platinum-doped TNN (Pt-TNN) interactions.

Initially, geometry optimizations were performed for the doped configurations, followed by single-point energy calculations. Subsequently, non-collinear (NCL) magnetic calculations were conducted to investigate the magnetic behavior of the systems. NCL calculations played a key role in achieving the primary objective of this study: analyzing magnetic materials for spintronic applications.

All calculations were performed using Density Functional Theory (DFT). The study included evaluations of formation energies, exchange energies, volume changes, charge density differences (CDD), and partial density of states (PDOS). These analyses provided a detailed understanding of the structural, electronic, and magnetic properties of the doped materials. Additionally, the influence of dopants on the lattice's stability and behavior was assessed, and potential application areas were suggested based on the findings.

SYMBOLS

$\boldsymbol{V_x}$: Vacancy of X atom or molecule

$\boldsymbol{X_{int}}$: Interstial of X atom

$\boldsymbol{E_{tot}}$: Total energy of many electron system

$\boldsymbol{\Psi}$: The many-body wave function of the system

$\boldsymbol{\hat{H}}$: Hamiltonian of the system

$\boldsymbol{\hat{T}}$: Kinetic energy

$\boldsymbol{\hat{Z}}$: Coloumb energy

$\boldsymbol{V_m}$: External potential energy

$\mathbf{r}_i$: Position vector of ith electron

$\boldsymbol{\nabla^2}$: Laplace operator

$\boldsymbol{F[X]}$: Functional of function X

$\langle$: Bra

$\rangle$: Ket

$\boldsymbol{E_{XC}}$: Exchange-correlation energy

$\boldsymbol{n(\mathbf{r})}$: Electron density

$\boldsymbol{n_o}$: Ground state electron density

$\boldsymbol{V_H}$: Hartree potential

$\boldsymbol{V_{tot}}$: Effective potential

$\boldsymbol{V_{XC}}$: Exchange-correlation potential

$\boldsymbol{\varepsilon_i}$: Eigen vectors

$\boldsymbol{\psi_i(\mathbf{r})}$: Eigen values

$\boldsymbol{c_i(\mathbf{G})}$: Plane-wave coefficients

$\mathbf{G}$: Reciprocal lattice vector

$\mathbf{G}_{max}$: Biggest reciprocal lattice vector in series expansion

$\boldsymbol{\varepsilon_{xc}}$: Exchange-correlation energy approximation

$\boldsymbol{E_{XC}^{LDA}}$: Exchange-correlation energy functional with local density approximation

E_{XC}^{GGA} : Exchange-correlation energy functional with generalized gradient approximation

E_{cut} : Cutoff energy

E_F : Fermi energy

E_{VBM} : Energy of the valence band maximum

$\vec{G}$: Reciprocal lattice vector

n_i : Number of atoms added or substracted

$\Delta H^{FE}(D)$: The formation energy of doped system

$E_{tot}(B)$: Total energy of the pristine supercell

$E_{tot}(D)$: Total energy of the doped supercell

E_f : Fermi level energy

E_{VBM} : Valence band maximum energy

E_{corr}^{q} : Finite size correction energy

ΔV : Potential alignment term

μ_i : Total chemical potential of atom/compound i

μ_i' : Energy of one atom/compound

$\Delta\mu_i$: Intrinsic chemical potential of atom/compound i

n_i : Number of kind i atoms removed from or added to the pristine structure

q : Charge

ABBREVIATIONS

AFM	: Antiferromagnetic
CBM	: Conduction Band Minimum
CDD	: Charge Density Difference
DFT	: Density Functional Theory
DOS	: Density of States
EF	: Fermi Energy
FA	: Formamidinium
$FAPbI_3$	: Formamidinium Lead Triiodide
FM	: Ferromagnetic
GGA	: Generalized Gradient Approximation
k-points	: Reciprocal Space Points
LDA	: Local Density Approximation
MD	: Molecular Dynamics
NN	: Nearest Neighbors
OUTCAR	: Output file from VASP containing detailed calculation results
PAW	: Projected Augmented Wave
PBE	: Perdew-Burke-Ernzerhof
PDOS	: Partial Density of States
PV	: Photovoltaics
SCF	: Self-Consistent Field
SP	: Single Point (Electronic structure calculation without relaxation)
TDOS	: Total Density of States
TNN	: Third Nearest Neighbors
VASP	: Vienna Ab initio Simulation Package
VBM	: Valence Band Maximum
XC	: Exchange - Correlation

LIST OF FIGURES

PAGE

1. INTRODUCTION

Despite remarkable progress in energy production technologies, the development of efficient and scalable energy storage solutions remains a significant challenge. The increasing demand for advanced energy storage systems stems from the necessity to support renewable energy infrastructures and next-generation devices with reliable and adaptable technologies. Additionally, the advent of next-generation electronic devices, autonomous systems, and the Internet of Things (IoT) creates a pressing demand for innovative storage technologies that are both reliable and adaptable. Within this context, hybrid organic–inorganic perovskites have attracted substantial attention due to their unique structural, optical, and electronic properties [4, 5]. These materials are particularly renowned for their versatility, which stems from the ability to integrate organic and inorganic components within a single lattice structure, offering exceptional tunability through various compositional modifications and doping strategies [6]. This adaptability not only enables the optimization of material properties for specific applications but also broadens the scope of potential functionalities, making hybrid perovskites a focal point in materials research.

The interplay between electronic and magnetic properties has received increasing attention, particularly in fields such as energy storage, spintronics, and magnetic sensing. Within this context, diluted magnetic semiconductors (DMS) have emerged as a key class of materials. These systems are formed by introducing magnetic dopants into non-magnetic semiconductor lattices, thereby combining tunable electronic conductivity with magnetism arising from the localized magnetic moments of the dopant atoms [7].

These materials combine the properties of semiconductors—such as tunable electronic conductivity—with magnetic behaviors imparted by doped magnetic atoms [7]. This dual functionality enables unique applications in spintronics, where electron spin, rather than charge, is exploited for information processing and storage. DMS materials exhibit spin-polarized electron transport and are considered ideal

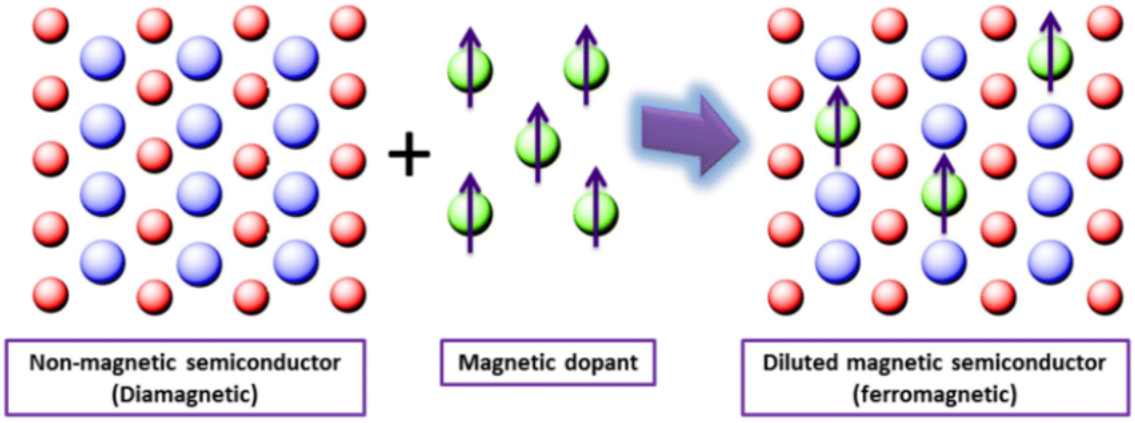

Figure 1.1 Formation mechanism of diluted magnetic semiconductors (DMS), illustrating the incorporation of magnetic dopants into a non-magnetic semiconductor (diamagnetic) lattice. The addition of magnetic dopants introduces localized magnetic moments, resulting in a ferromagnetic DMS material with combined magnetic and semiconducting properties. [1]

candidates for devices such as spin transistors, spin filters, and magnetic sensors. Their magnetic and electronic characteristics can be precisely tuned by modifying doping concentration, temperature, and external magnetic fields, allowing for flexible control in advanced technologies.

Furthermore, magnetic and semiconductor-based devices differ significantly in their charge transport mechanisms. While magnetic materials typically show low resistivity at room temperature, undoped or moderately doped semiconductors exhibit much higher resistivity under the same conditions [8]. This contrast arises mainly from the formation of a depletion layer at the interface between the semiconductor and a metallic contact, which can vary in thickness from a few nanometers to several micrometers depending on the material and doping level [9].

Two key parameters govern the performance of spintronic devices and systems: spin polarization and doping density. Spin polarization dictates the efficiency of spin-polarized electron transport, while doping density affects both the resistivity and spin diffusion length of the material [9]. In addition to carrier-based mechanisms, spin transport can also occur via magnons—the fundamental quanta of spin waves. These characteristics open up new possibilities for designing advanced materials that integrate magnetic and semiconducting functionalities, thereby paving the way for

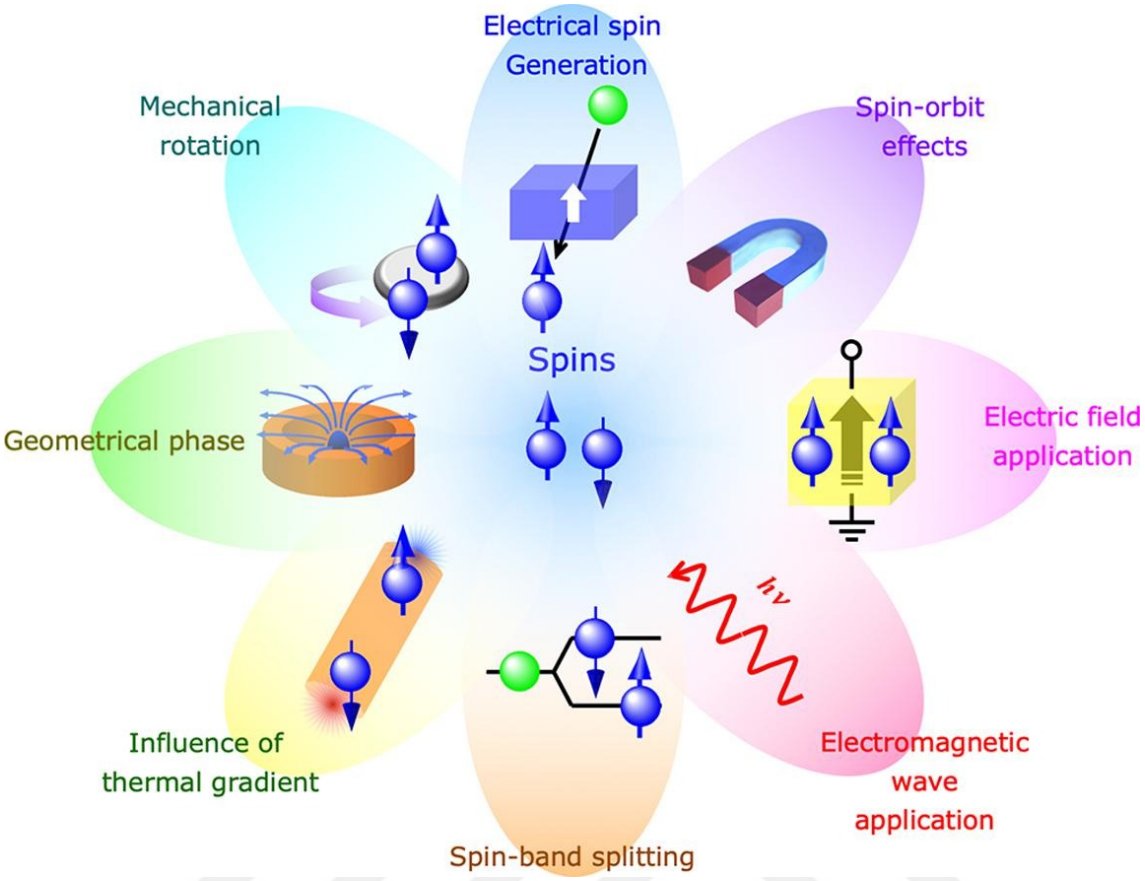

Figure 1.2 Schematic diagram of major methods to generate a spin-polarised current. [2]

next-generation energy storage and spintronic technologies.

Formamidinium lead triiodide ($FAPbI_3$), a prominent member of the hybrid perovskite family, is particularly notable for its ability to transition between cubic, tetragonal, and orthorhombic structural phases under varying conditions.

These phase transitions not only influence the electronic and optical properties of $FAPbI_3$ but also have a substantial impact on its performance in energy storage and magnetic applications [10]. However, the pristine $FAPbI_3$ phase is inherently unstable under environmental conditions, which necessitates structural modifications to improve its durability and functionality.

Recent advances in doping techniques have demonstrated that $FAPbI_3$ can be tailored for specific applications. Replacing lead (Pb) atoms with transition metals or rare-earth elements introduces localized magnetic moments, allowing for a more

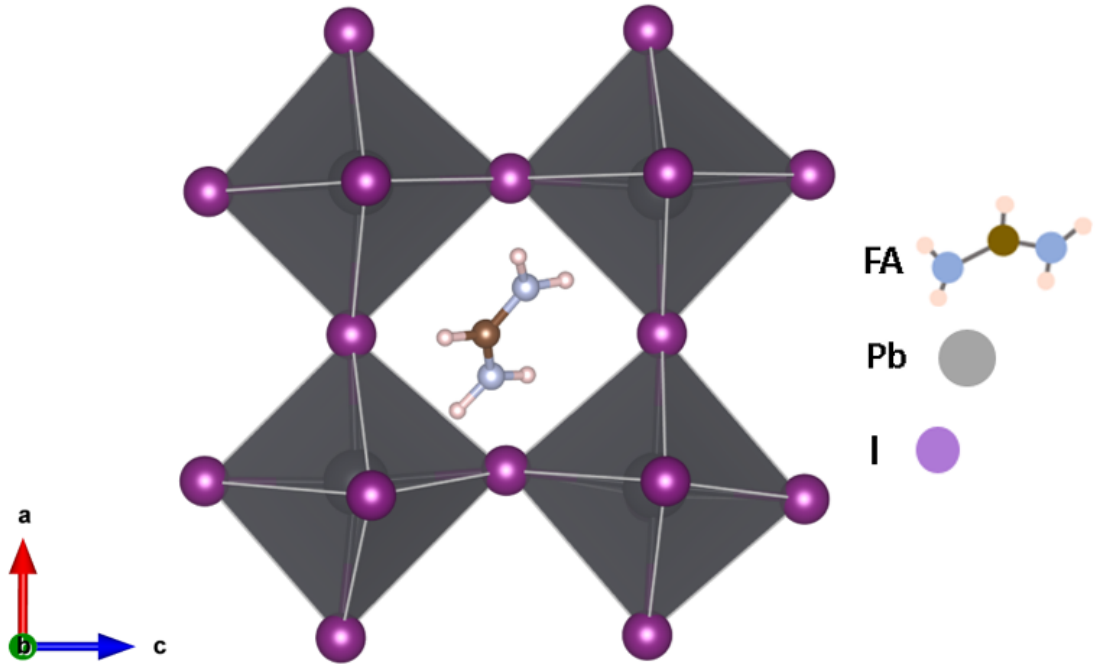

Figure 1.3 Crystal structure of $FAPbI_3$ perovskite in cubic phase.

in-depth investigation of the material's magnetic properties [10]. These dopants not only modulate the magnetic behavior but also significantly enhance charge transport and energy storage capabilities. In addition, the incorporation of electron carriers such as bismuth (Bi) and platinum (Pt) at third-nearest-neighbor (TNN) sites further improves the material's potential for energy-related applications.

Although diluted magnetic semiconductors (DMS) have been widely studied for their promising properties and applications, this study does not claim the realization of DMS behavior. Instead, it focuses on exploring the magnetic and electronic properties of doped hybrid perovskite structures, aiming to contribute to the development of candidate materials for spintronic technologies.

This work systematically investigates doped $FAPbI_3$ structures to evaluate their potential in energy storage and spintronic applications. Using Density Functional Theory (DFT), we analyze the structural, electronic, and magnetic properties of these materials in detail. Particular emphasis is placed on the effects of nearest-neighbor (NN) and third-nearest-neighbor (TNN) dopants, as they play a critical role in shaping the overall behavior of the system. To achieve this, advanced compu-

tational techniques—including non-collinear magnetic calculations, charge density difference (CDD) analysis, and partial density of states (PDOS) evaluations—are employed.

By examining the effects of transition metal and rare-earth element doping, we aim to establish new design principles for hybrid perovskite-based materials that exhibit enhanced magnetic functionality alongside optimized electronic performance. These insights are expected to contribute to the development of multifunctional materials capable of addressing the dual challenges of energy storage and magnetic device innovation, thereby paving the way for advancements in next-generation technologies.

2. METHODS

In this section, we present a comprehensive overview of the methodologies employed in this study, aimed at systematically exploring the structural, electronic, and magnetic properties of doped $FAPbI_3$-based hybrid perovskites. The primary computational framework utilized in our investigation is DFT, a widely acknowledged and robust approach for simulating the quantum mechanical behavior of materials. DFT enables precise calculations of the electronic structure, energy states, and interactions within complex materials, making it particularly suitable for studying hybrid perovskite systems with diverse doping configurations. To achieve our objectives, a series of calculations were performed to evaluate the formation energies, exchange energies, and structural stability of twenty-four distinct atomic configurations. These configurations were carefully designed to capture the effects of substituting Pb atoms with various transition metals and rare-earth elements, as well as the inclusion of electron carriers such as Bi and Pt at specific lattice sites. By systematically varying the dopants and their positions within the lattice, we aimed to uncover trends in magnetic and electronic behavior, with a focus on identifying promising candidates for spintronic applications.

Key aspects of the analysis include the evaluation of the PDOS and CDD. The PDOS calculations provide detailed insights into the electronic states and their contributions to the overall density of states, allowing us to investigate the impact of doping on the band structure and energy levels. The CDD analysis, on the other hand, offers a visualization of charge redistribution caused by dopants, highlighting localized and delocalized interactions within the material.

To ensure the reliability of our findings, advanced computational techniques, such as non-collinear magnetic calculations, were employed to account for the influence of spin-orbit coupling and magnetic anisotropy. These calculations are critical for accurately modeling the magnetic properties of doped structures, particularly in cases where complex interactions between magnetic moments are present. Additionally, geometric optimization and single-point energy calculations were performed to assess the structural stability and energy minima of each configuration.

The methodologies adopted in this work are designed to provide a holistic understanding of the interplay between structural modifications and the resulting electronic and magnetic properties of hybrid perovskites. Detailed descriptions of the computational parameters, such as exchange-correlation functionals, plane-wave cutoffs, and k-point sampling, are provided in the subsequent sections to ensure reproducibility and transparency. This systematic approach aims to contribute valuable insights into the rational design of high-efficiency spintronic materials, paving the way for the development of advanced multifunctional devices.

Finally, the methodologies outlined in this section will be further elaborated upon in the following sections, with each computational method described in greater detail under specific headings.

2.1. Density Functional Theory

A material's electronic architecture is vital for gaining insights into its behavior and for facilitating improvements. Analyzing the ground-state electron configuration

provides insights into the material's stability, insulating properties, and behavior. Therefore, the accurate analysis of electronic structure is critical for both fundamental and applied sciences. Quantum mechanics can describe the properties of a system using the Schrödinger equation; however, for multi-body systems, the resulting equation becomes mathematically complex and nearly impossible to solve or interpret [3, 11].

DFT simplifies this complexity by adopting the electron density approach instead of the wave function, making the expression more straightforward and comprehensible. Consequently, mathematical computations are significantly eased, and the interpretation of the results becomes more accessible.

In this study, DFT has been chosen as the primary computational method to obtain the electronic properties of our materials with the highest possible accuracy and efficiency. As a quantum mechanical approach, DFT calculates the total energy and electronic structure of multi-body systems by focusing on electron density. Additionally, DFT is a low-cost and time-efficient method.

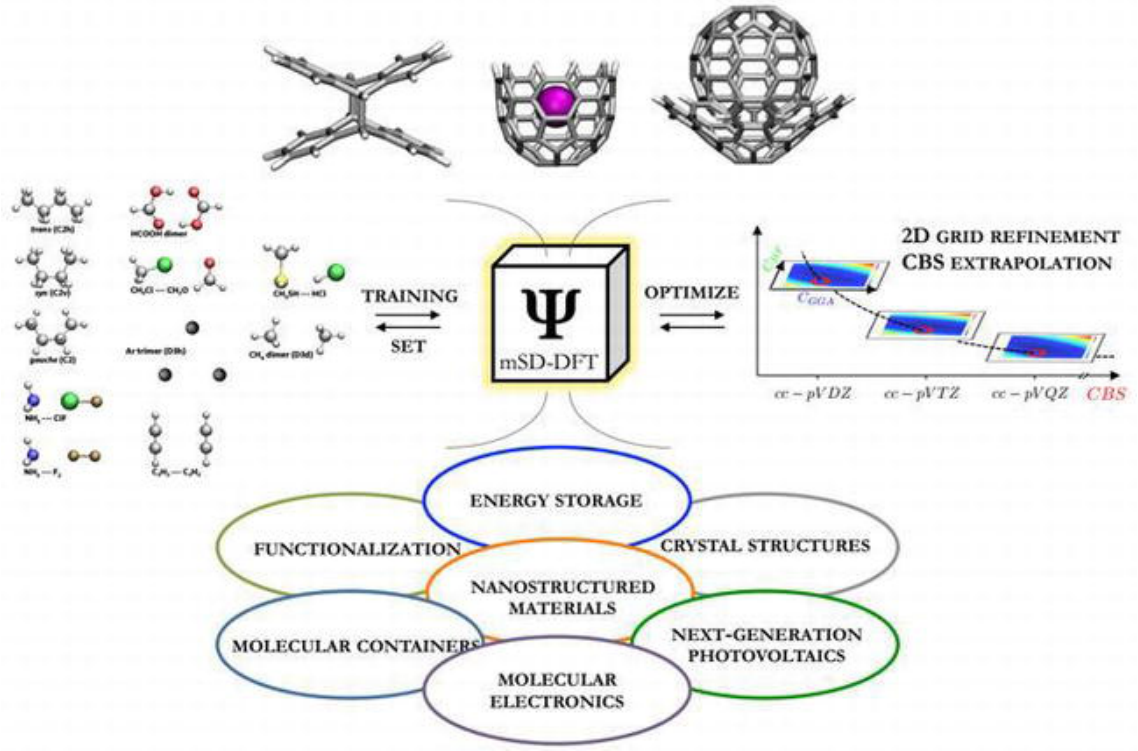

Figure 2.1 Application areas of DFT [3]

The theoretical foundations of this approach are based on the Hohenberg-Kohn theorems introduced in 1954 [12]. The Hohenberg-Kohn theorems demonstrated that the ground-state electron density influences all properties of a system in the absence of a magnetic field. The introduction of the Kohn-Sham equation, as a single-particle independent Schrödinger equation, transformed the many-body Schrödinger equation into a computationally feasible form. In light of these advancements, Walter Kohn was awarded the Nobel Prize in 1998, once again highlighting the significance of DFT as a crucial approach in materials science [13]

The success of DFT lies in the development of exchange-correlation functionals that accurately model complex many-body interactions. These functionals enable precise predictions of molecular structures, bond dissociation energies, and other quantum properties. However, the reliance of exchange-correlation functionals on approximate computational methods brings certain limitations to DFT. To overcome these limitations, ongoing advancements such as highly detailed functionals and empirical dispersion corrections continue to be developed [14]. These innovations aim to enhance the reliability of DFT for a broader range of materials.

The aggregate energyE_{tot} of a many-electron system can be calculated using Equation 2.1, where K is the kinetic energy, U_{ext} represents the energy due to the electrons' movement in an external potential field, C indicates the Coulomb interaction, and $\hat{H}$, is the Hamiltonian, of the system is :

$$H = K + U_{ext} + C \tag{2.1}$$

Quantum mechanically the factors can be defined :

$$K = \frac{1}{2}\int [\nabla\Psi^*(r)\nabla\Psi(r)]dr\Psi^*(r^{'}) \tag{2.2}$$

$$U = \int [u(r)\Psi^*(r)\Psi(r)]dr \tag{2.3}$$

$$C = \frac{1}{2}\int \frac{\Psi^*(r^{'})\Psi^*(r)\Psi(r^{'})\Psi(r)}{\left|r - r^{'}\right|}drdr^{'} \tag{2.4}$$

The solution of Hamiltonian from equation 2.1 :

$$\hat{H}\Psi(\mathbf{r}_1, ..., \mathbf{r}_N) = E\Psi(\mathbf{r}_1, ..., \mathbf{r}_N) \tag{2.5}$$

The formulation of a many-body system within the context of Hamiltonian mechanics can be articulated as:

$$\hat{H}^{'}\Psi^{'} = E^{'}\Psi^{'} \tag{2.6}$$

According to the variational principle, the ground-state wave function $\Psi(r)$ gives the lowest possible energy of the system. The principle asserts that no wave function can produce an energy that is below that of the ground state; this can be defined as:

$$\langle\Psi|\hat{H}|\Psi\rangle = \langle\Psi^{'}|\hat{H}|\Psi^{'}\rangle \tag{2.7}$$

where,

$$E_{tot} = \langle\Psi|\hat{H}|\Psi\rangle \tag{2.8}$$

Utilizing the fundamental characteristic of the ground state:

$$\langle\Psi^{'}|\hat{H}|\Psi^{'}\rangle = \langle\Psi|\hat{H}^{'}|\Psi\rangle + \int [u(r) - u^{'}(r)]\rho(r)dr \tag{2.9}$$

$$\langle\Psi|\hat{H}^{'}|\Psi\rangle = \langle\Psi^{'}|\hat{H}|\Psi^{'}\rangle + \int [u^{'}(r) - u(r)]\rho(r)dr \tag{2.10}$$

And by using the above equations, we finally obtain:

$$E + E^{'} < E^{'} + E \tag{2.11}$$

The functional relationship between the minimum energy state and the corresponding density is expressed as:

$$E|\rho(r)| = K|\rho(r)| - U|\rho(r)| + C|\rho(r)| \tag{2.12}$$

2.2. Exchange - Correlation Functionals

In this section, we will discuss some of the foundations and limitations that paved the way for modern DFT. In 1929, Bloch was the first to mention the exchange contribution, which later became recognized through Monte Carlo simulations of uniform gases. Kohn and Sham introduced the concept that the exchange-correlation functional at any given point in space is determined exclusively by the spin density present at that specific location, referring to this methodology as the Local Density Approximation (LDA). [13].

$$E_{xc}^{LDA}[n] = \int \varepsilon_{xc}(n) n(\mathbf{r})\, d^3\mathbf{r} \tag{2.13}$$

The LDA functional depends exclusively on the local density at the location where the functional is evaluated. While it provides geometrically accurate results, it overbinds atoms and molecules by approximately 1 eV per bond, leading to incorrect predictions for thermochemistry.

By incorporating terms dependent on density gradients, a new approach called the Generalized Gradient Approximation (GGA) was developed.

$$E_{xc}^{GGA}[n] = \int \varepsilon_{xc}(n, \nabla n) n(\mathbf{r})\, d^3\mathbf{r} \tag{2.14}$$

As shown in the figure, functional models such as PW86 and PW91 emerged from this approach, with PW91 achieving significant accuracy for binding energies of approximately 6-10 kcal/mol in 1993. Today, the PBE functional is the most widely used GGA for solids in materials science, while BLYP and Lee-Yang-Parr are the most common correlation functionals in chemistry [15].

Over time, new approaches were developed by incorporating additional physical parameters. For example, a hybrid GGA combines a standard GGA with a Hartree-Fock component, also including kinetic energy density to define the GGA component. These components are found in a meta-hybrid, while a double-hybrid incorporates contributions from second-order Møller-Plesset perturbation theory into

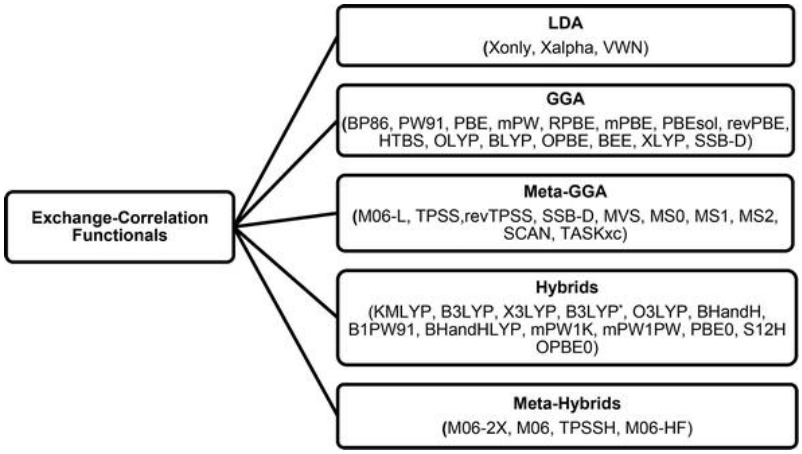

Figure 2.2 Commonly used Exchange-Correlation Functions. [3]

its hybrid or meta-hybrid components. Traditional GGA functionals like PBE often overlook Van der Waals interactions [16, 17].

The framework of DFT usually includes contributions from GGA, LDA, Hartree-Fock exchange, and hybrid approaches, along with aspects of meta-GGA — all of which together constitute what is known as the exchange-correlation (XC) functional. [18].

2.3. Calculation of Formation Energy

The stability of additive-containing hybrid perovskite structures was evaluated by calculating their formation energies, providing insights into their thermodynamic favorability under different configurations. The formation energy is defined as the difference between the total energy of the doped structure and the cumulative energies of its individual components in their respective reference states (e.g., Pb in its metallic phase, I_3 molecule for iodine, and the elemental form of the substituted dopant atoms). These calculations were performed for crystal structures subjected to varying environmental conditions. Structures with lower formation energies are considered more thermodynamically stable, as a smaller energy difference implies a higher probability of preserving structural integrity. In contrast, higher formation energies indicate reduced thermodynamic stability. In order to evaluate the impact

of dopant atoms on the structural stability of hybrid perovskites, the formation energy was computed based on the following formula [10, 19]:

$$E_f = E_{\text{tot}}^{\text{doped}} - E_{\text{tot}}^{\text{pristine}} - \sum_i n_i \mu_i + q(E_F + E_{VBM} + \Delta V) + E_{\text{corr}}^q \tag{2.15}$$

In this context, $E_{\text{tot}}^{\text{doped}}$ represents the total energy of the supercell after doping, calculated using DFT. $E_{\text{tot}}^{\text{pristine}}$ denotes the total energy of the undoped reference supercell. To ensure a consistent comparison between these two systems, correction terms involving atomic reservoirs are introduced. These account for differences in chemical composition by incorporating the chemical potentials (μ_i) of atoms added to or removed from the system. The term $q(E_F+E_{VBM}+\Delta V)$ is included for charged configurations, where q is the charge state, E_F is the Fermi level referenced to the valence band maximum (E_{VBM}), and ΔV accounts for potential alignment. E_{corr}^q represents the correction for finite-size effects in charged supercells. The obtained formation energies not only serve as a basis for discussing the electronic and magnetic properties in the following sections, which are closely related to structural stability, but also provide a significant perspective for evaluating the energetic feasibility of dopant incorporation under various structural and environmental conditions.

2.4. Partial Density of States

In this study, PDOS was employed as a critical computational tool to analyze the contribution of individual atoms and orbitals to the overall electronic structure of the system [20]. PDOS is derived by decomposing the Total Density of States (TDOS) into specific atomic and orbital contributions, providing a fine-grained understanding of the electronic environment within the material. To provide a theoretical basis, PDOS can be formally expressed as [21]:

$$D_i(E) = \sum_n \int |\langle \phi_i | \psi_n(\mathbf{r}) \rangle|^2 \, \delta(E - E_n) \, d\mathbf{r} \tag{2.16}$$

Here, $D_i(E)$ represents the PDOS projected onto the atomic orbital ϕ_i, and ψ_n

denotes the Kohn–Sham eigenstates with eigenenergies E_n. The projection quantifies the contribution of a specific atomic orbital to each electronic state, which is essential for identifying orbital interactions and localized states introduced by dopants.

This method allows us to investigate the localized and delocalized nature of electronic states, which is particularly important in doped systems where the electronic configuration can vary significantly based on the dopants and their positions within the lattice [22, 23].

By analyzing PDOS, we were able to evaluate how the introduction of transition metals and rare-earth elements as dopants influences the electronic structure of $FAPbI_3$. Specifically, this approach highlights changes in the density of states around the Fermi level, which directly impacts the material's electronic conductivity, band gap, and potential for spin-polarized transport. Furthermore, the PDOS data were used to identify key orbital interactions, such as hybridization effects between dopant orbitals and the host lattice orbitals, which play a crucial role in modifying the material's electronic behavior [24, 25].

The orbital-resolved PDOS analysis provided insights into the role of d and f states [26], especially in the presence of transition metal and rare-earth dopants.

The electronic structure and PDOS calculations were performed using the Vienna Ab initio Simulation Package (VASP) within the framework of DFT. The Perdew–Burke–Ernzerhof (PBE) functional within the GGA was used to describe the exchange-correlation interactions. PDOS was obtained by projecting the Kohn–Sham wave functions onto atomic orbitals using the projection scheme implemented in VASP. This approach allows the decomposition of the total density of states into orbital-resolved contributions, such as s, p, d, and f states, enabling detailed analysis of the electronic characteristics of individual atomic sites [27]. All PDOS calculations were conducted after full geometric optimization of the doped supercells, ensuring that the electronic structure reflects the relaxed ground-state configuration of the material.

The results were further validated by comparing the total PDOS with the TDOS to confirm consistency in the electronic density distribution. In addition, a thorough comparison between doped and undoped configurations was conducted to isolate the effects of specific dopants on the electronic structure. By correlating the PDOS data with other computational results, such as CDD and non-collinear magnetic calculations, we were able to build a comprehensive understanding of the interplay between electronic structure and magnetic behavior in doped $FAPbI_3$ perovskites. These findings underline the importance of PDOS as a powerful tool in the rational design of advanced materials for spintronic and energy storage applications [28].

2.5. Charge Density Difference

In this study, CDD analysis was employed as a fundamental tool to investigate the redistribution of electronic density in doped $FAPbI_3$-based hybrid perovskite structures. CDD offers a quantitative and visual means to understand how charge density is reallocated in response to doping and the incorporation of specific elements. It is particularly valuable for identifying changes in charge distribution caused by atomic substitution, chemical bonding, and the interaction of localized electronic states within the lattice [29].

The CDD is mathematically defined as the difference between the total charge density of the system, $\rho_{\text{total}}(r)$, and the sum of the charge densities of its individual components in their isolated states, $\rho_{\text{components}}(r)$ [12]:

$$\Delta\rho(r) = \rho_{\text{total}}(r) - \sum \rho_{\text{components}}(r) \tag{2.17}$$

Here, $\rho_{\text{total}}(r)$ represents the electronic density of the fully relaxed doped structure, while $\rho_{\text{components}}(r)$ corresponds to the superposition of charge densities of the isolated atomic or molecular fragments. This decomposition allows for the visualization of charge accumulation and depletion regions, which are crucial for understanding the nature of bonding and electronic interactions within the material.

The theoretical basis of CDD analysis is rooted in DFT, which enables an accurate representation of charge distribution in complex systems. In this work, CDD calculations were carried out using a plane-wave basis set within the projector-augmented wave (PAW) framework, as implemented in the VASP [22,26]. Exchange-correlation interactions were described using the PBE functional within the GGA. All charge density computations were performed after full structural optimization to ensure consistency with the ground-state configuration.

The CDD results revealed significant regions of charge accumulation and depletion around the dopant sites, indicating strong localized interactions and modifications in the bonding environment [25, 30]. Charge accumulation typically occurred near the dopant atoms, suggesting the formation of stronger bonding interactions or the presence of localized electronic states that enhance stability. In contrast, charge depletion was often observed around host lattice atoms, reflecting charge transfer from the host to the dopant.

These redistribution patterns provide insights into how dopants alter the electronic structure, influencing properties such as band alignment, charge transport, and magnetic interactions. Furthermore, CDD analysis highlights the formation of new bonding states and hybridized orbitals between dopants and the host lattice, which are critical for tailoring material functionality. This method is particularly effective in elucidating the role of dopants in hybrid perovskites designed for energy storage and spintronic applications.

By identifying regions of electronic charge redistribution, CDD analysis in this study underscores the fundamental role of doping in modifying structural and electronic behavior. The findings contribute to a deeper understanding of how charge localization and chemical bonding collectively influence the functional properties of the material. [31–33].

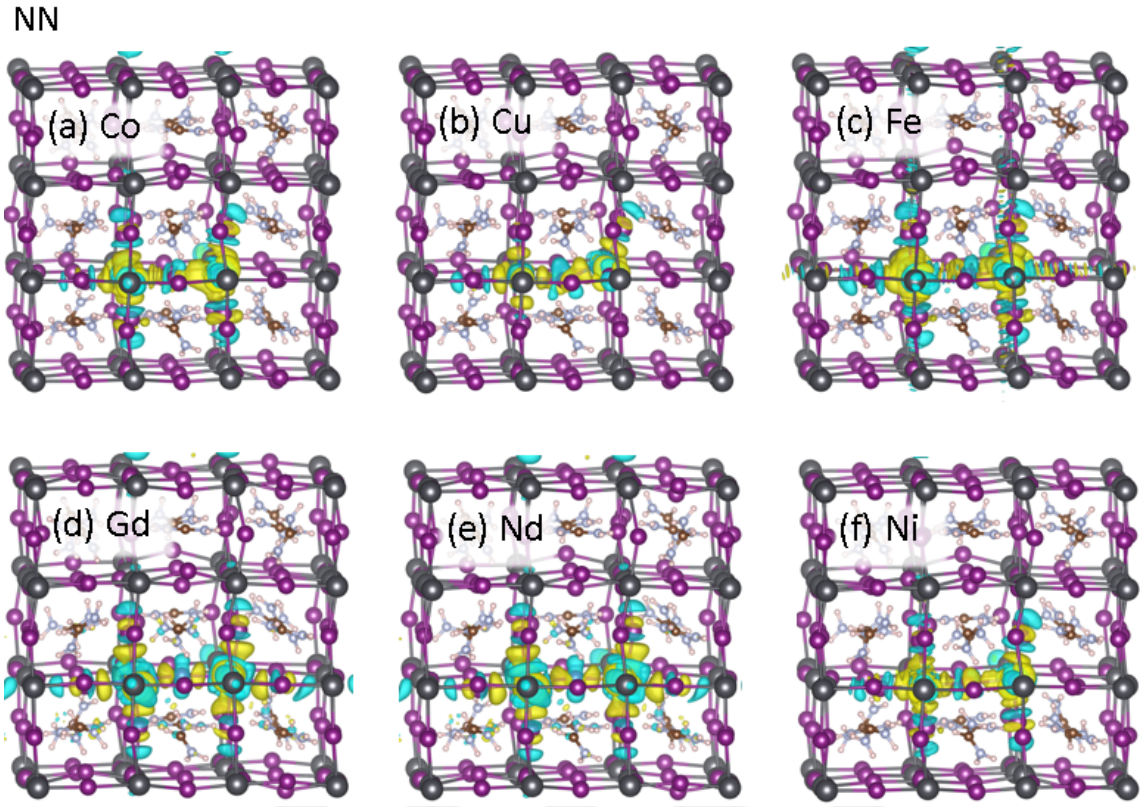

Figure 2.3 Charge density difference maps of Nearest Neighbors configurations

In Figure 2.3, the NN configuration illustrates the substitution of Pb atoms in the $FAPbI_3$ supercell with selected transition metals and rare-earth elements at NN positions. This configuration was designed to probe the localized electronic and structural effects induced by dopant incorporation. Through PDOS and CDD analyses, the resulting changes in charge redistribution and bonding interactions were systematically examined. The charge density difference maps clearly reveal the influence of each dopant on the immediate atomic environment, providing insights into electronic localization, potential bonding enhancement, and structural stabilization mechanisms.

Figure 2.4 illustrates the TNN configuration, in which Pb atoms in the $FAPbI_3$ supercell are replaced with selected transition metals placed at third-nearest-neighbor positions. This setup was designed to investigate the long-range electronic effects of dopants beyond the immediate coordination environment. In particular, the analysis aims to capture how such substitutions influence both structural and electronic properties without introducing significant local distortions.

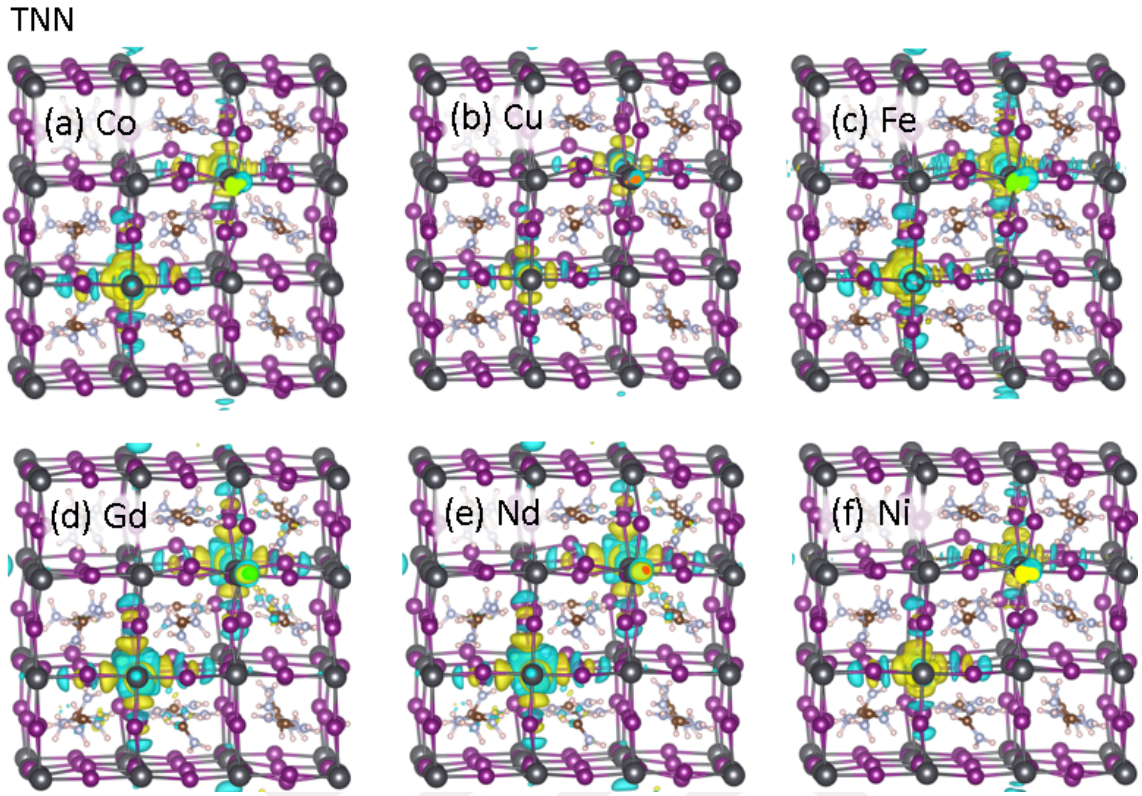

Figure 2.4 Charge density difference maps of Third Nearest Neighbors configurations

Formation energy and CDD analyses were employed to evaluate the extent of electronic redistribution and the stability of the system under these extended dopant configurations. This approach allows for a comprehensive understanding of the broader electronic interactions induced by dopants and their implications for material functionality.

By comparing the NN and TNN configurations, it becomes possible to distinguish the localized effects of dopants from their longer-range electronic influences. While NN substitution reveals immediate charge redistribution and bonding modifications around the dopant sites, the TNN configuration highlights the extended electronic interactions that propagate through the lattice, offering a broader perspective on how dopants affect the material's overall electronic and structural behavior.

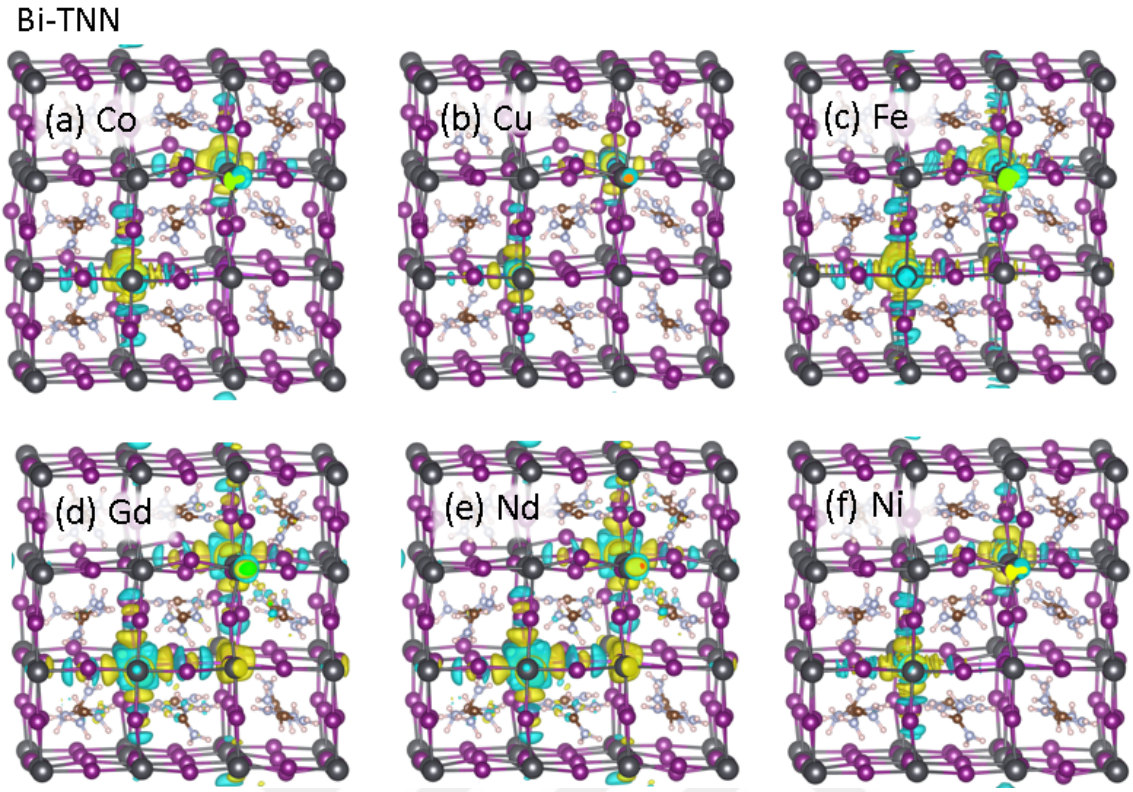

Figure 2.5 Charge density difference maps of Third Nearest Neighbors with Bismuth configurations

Figure 2.5 presents the Bi-TNN configuration, in which Bi atoms were incorporated into TNN positions to act as electron donors within the lattice. This configuration was designed to examine the influence of Bi on charge redistribution and its contribution to the electronic characteristics of the system. The primary objective was to understand how Bi alters the local electronic environment, potentially stabilizing the doped structure and enhancing carrier availability. CDD analysis was employed to reveal the redistribution patterns induced by Bi doping, providing insights into its role in modulating the electronic behavior of hybrid perovskites.

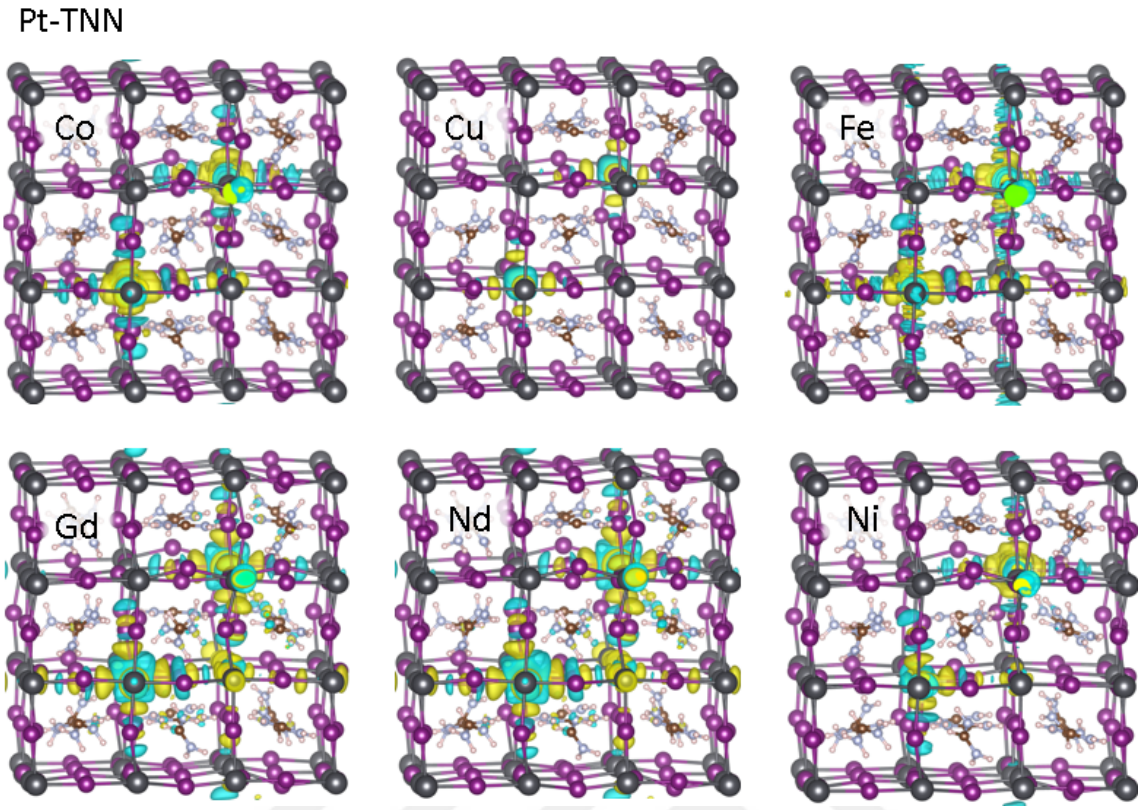

Figure 2.6 Charge density difference maps of Third Nearest Neighbors with Platinum configurations

Figure 2.6 illustrates the Pt-TNN configuration, where Pt atoms were introduced at third-nearest-neighbor positions to act as electron donors and enhance carrier dynamics within the lattice. This configuration was employed to evaluate the influence of Pt doping on the electronic structure, with particular focus on charge redistribution and bonding modifications.

Using PDOS and CDD analyses, the electronic interactions between Pt atoms and the surrounding host lattice were systematically examined. These analyses provided insights into the role of Pt in modulating charge localization and contributing to the overall electronic behavior of the doped perovskite system.

A comparative analysis of the Bi-TNN and Pt-TNN configurations reveals distinct behaviors in charge redistribution and electronic interaction patterns. Bi, due to its electronic structure, tends to induce stronger charge accumulation in localized regions, suggesting enhanced bonding interactions and potential stabilization of the

surrounding lattice. In contrast, Pt exhibits a more delocalized charge distribution, which may contribute to increased carrier mobility and dynamic interaction with the host structure. While both elements act as electron donors, their differing impacts highlight the importance of electronic configuration in determining the dopant–host coupling and resulting material functionality.

By comparing all four configurations NN, TNN, Bi-TNN, and Pt-TNN—a comprehensive understanding of dopant-induced modifications emerges. NN arrangements emphasize localized effects, with strong electronic interactions concentrated near the dopant sites. TNN configurations extend the scope to long-range electronic influence, revealing how dopants alter the lattice without significantly disturbing the immediate structure. The inclusion of Bi and Pt as electron carriers in TNN environments further demonstrates how auxiliary elements can be used to fine-tune the charge landscape, hybridization behavior, and potential conductivity pathways. Together, these configurations provide a multi-scale perspective on doping strategies for tailoring the electronic and structural properties of hybrid perovskites.

2.6. Configurations with Dopants

In this study, the $FAPbI_3$ structure was systematically doped with transition metals and rare-earth elements to investigate their effects on the material's electronic properties. The doping strategy focused on four distinct scenarios: NN, TNN, and two extended TNN variants involving additional electron carriers—Bi-TNN and Pt-TNN—where bismuth and platinum were introduced to act as electron donors. Each configuration was designed to explore the interactions between dopants and the $FAPbI_3$ lattice, offering a comprehensive understanding of the material's structural, magnetic, and electronic behavior.

For the NN configuration, two Pb atoms, identified as nearest neighbors within the lattice, were substituted with selected transition metals, including cobalt, copper, iron, gadolinium, neodymium, and nickel. This approach aimed to examine

localized interactions and their influence on the material's stability and magnetic properties.

The TNN configuration extended the analysis to TNN positions, where two Pb atoms were replaced with the same set of transition metals. This setup was designed to study long-range interactions and their impact on the electronic structure, stability, and magnetic characteristics of the material.

To further explore the role of electron carriers, additional doping was introduced into the TNN configuration. In the Bi-TNN scenario, one of the third-nearest-neighbor Pb atoms was replaced with bismuth, while in the Pt-TNN scenario, platinum was introduced for the same purpose. These configurations enabled the investigation of how electron-carrying elements influence charge distribution, bonding interactions, and overall electronic and magnetic behavior within the material.

For each of the six transition metals, separate structures were prepared for all four scenarios—NN, TNN, Bi-TNN, and Pt-TNN. This systematic approach provided a detailed framework for understanding the interplay between different dopants and their respective roles in modifying the properties of $FAPbI_3$. All configurations were fully relaxed through geometric optimization to ensure consistency with the ground-state structure before electronic and magnetic analyses were performed. Additionally, spin-polarized calculations were employed to properly capture the magnetic contributions of transition metal dopants.

2.7. Computational Details

All first-principles calculations in this study were performed using the VASP, based on DFT [26]. For each configuration, a $3 \times 3 \times 3$ cubic supercell of $FAPbI_3$ was constructed using the Visualization for Electronic and Structural Analysis (VESTA) software [34]. Electronic exchange-correlation interactions were described using the PBE functional. This functional, developed by PBE, belongs to the GGA family [15]. The interactions between valence electrons and the ionic core were treated using the

PAW method [35]. A Gamma-centered $2 \times 2 \times 2$ k-point mesh was employed for Brillouin zone sampling. The plane-wave kinetic energy cutoff was set to 400 eV for all calculations [36].

Geometry optimization was carried out while keeping the lattice volume fixed, allowing atomic positions to relax until the Hellmann–Feynman forces on each atom were less than 0.01 eV/Å. The energy convergence criterion was set to a sufficiently low threshold to ensure accurate total energy calculations. POTIM parameters were tested and optimized prior to final calculations.

Post-processing analyses were performed using VASP output files. PDOS and band structure data were extracted and visualized using Origin software. These plots provided insight into the electronic structure and bandgap characteristics of the doped configurations, ensuring high clarity and analytical precision.

3. RESULTS

3.1. Structural Characterization

The graphs presented in Figure 3.1 illustrate the formation energies (in eV) for various dopants (Co, Cu, Fe, Gd, Nd, and Ni) within different doping configurations: NN, TNN, bismuth-doped TNN (Bi-TNN), and platinum-doped TNN (Pt-TNN).

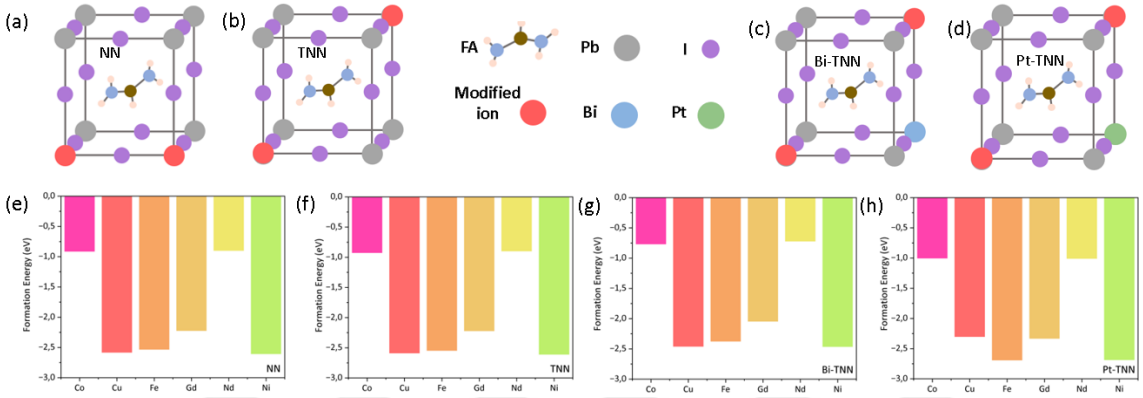

Figure 3.1 (a–d) display the schematic representations of the four doping configurations, while (e–h) present the corresponding formation energies.

The analysis of formation energies reveals notable trends in the stability of dopants within the $FAPbI_3$ lattice. Gd demonstrates superior stability in the NN configuration, suggesting its strong localized bonding interactions with adjacent lattice atoms. This behavior highlights gadolinium's strong capacity to enhance lattice cohesion when substituted at adjacent lead sites.

On the other hand, Cu demonstrates a significant improvement in stability in the TNN configuration compared to NN. This behavior suggests that copper's influence extends to longer-range interactions, promoting more uniform charge distribution and mitigating structural distortions in the TNN configuration.

These observations offer valuable insights into the potential magnetic properties of the doped structures. The ability of gadolinium and copper to stabilize the lattice in various configurations highlights their potential to induce localized magnetic mo-

ments within the material. This magnetic behavior is crucial for the development of magnetic semiconductors, where controlled magnetic and electronic properties are vital for spintronic applications.

Specifically, gadolinium's magnetic behavior in NN configurations and copper's stabilization effects in TNN configurations provide opportunities for designing hybrid perovskite materials with tailored magnetic properties. By optimizing the doping strategy, it may be possible to achieve materials with improved magnetic ordering and spin-polarized electron transport, both of which are essential for advanced spintronic applications.

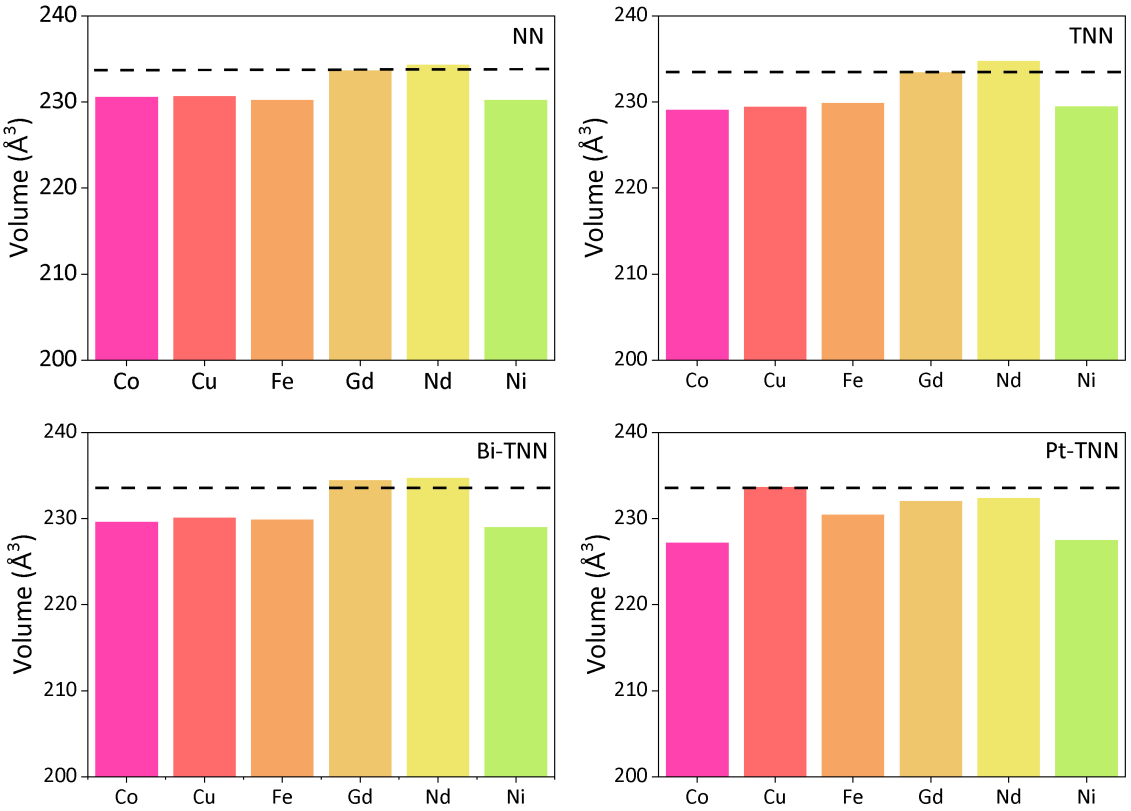

Figure 3.2 Volume change for NN, TNN, Bi-TNN, Pt-TNN

The volume analysis of the doped $FAPbI_3$ structures, as depicted in Figure 3.2, provides complementary insights into the structural stability trends observed in the formation energy analysis. Overall, the volume trends align with the formation energy results, indicating that dopants with minimal lattice distortion (as seen in volume analysis) also tend to have lower formation energies, contributing to higher

structural stability. This complementary relationship underscores the importance of combining these analyses for a comprehensive understanding of dopant behavior in hybrid perovskites.

In conclusion, the analysis of formation energies and volume changes reveals significant insights into the stability and magnetic properties of doped $FAPbI_3$. Dopants like gadolinium and copper play a crucial role in enhancing the structural cohesion and magnetic behavior of the material. The observed relationship between formation energy and volume suggests that minimizing lattice distortion is key to achieving high stability. These findings emphasize the importance of optimizing doping strategies for future research into advanced, multifunctional hybrid perovskites with potential applications in spintronics and energy devices.

3.2. Magnetic Characterization

The exchange energy values presented in Figure 3.3 highlight the magnetic interactions introduced by the dopants in the $FAPbI_3$ lattice. These values provide insights into the spin alignment tendencies and overall magnetic stability of the doped configurations.

Negative exchange energies, as observed in the doped $FAPbI_3$ configurations, indicate strong antiferromagnetic interactions, while positive values suggest a tendency toward ferromagnetism. Notably, Gd and Cu stand out in this analysis, with Gd exhibiting a marked antiferromagnetic behavior in the NN configuration, while copper demonstrates a pronounced ferromagnetic tendency in the TNN configuration. These results are consistent with previous findings and underscore the role of specific dopants in stabilizing distinct magnetic ordering.

In conclusion, the analysis of exchange energy values reveals the key role that dopants like gadolinium and copper play in determining the magnetic properties of $FAPbI_3$. Gd stabilizes antiferromagnetic ordering in NN configurations, while Cu stabilizes ferromagnetic ordering in TNN configurations. These findings open path-

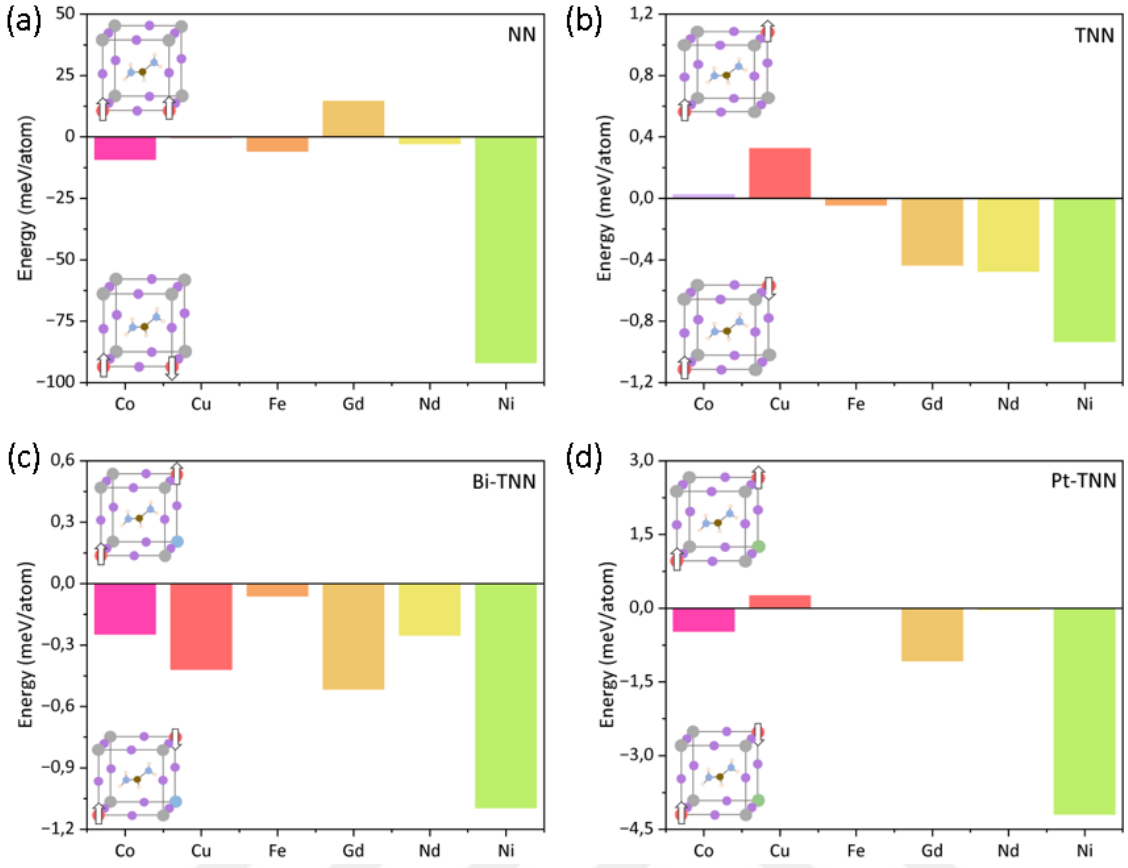

Figure 3.3 Exchange energy values for the doped $FAPbI_3$ configurations: NN, TNN, Bi-TNN, and Pt-TNN. The negative and positive exchange energy values are indicative of the antiferromagnetic and ferromagnetic interactions, respectively, that are introduced by the doping elements.

ways for tailoring magnetic behavior in hybrid perovskites by strategically selecting dopants and doping configurations.

3.3. Electronic Characterization

A more detailed investigation into the electronic structure of the surfaces was conducted through PDOS calculations, as depicted in Figure 3.4. The analysis of PDOS graphs reveals significant trends in the interactions within the $FAPbI_3$ lattice. In the NN interactions, the substitution of Cu atoms successfully maintains the structural and electronic integrity of the system. This indicates that Cu integrates harmoniously into the lattice and optimizes localized bonding interactions within the

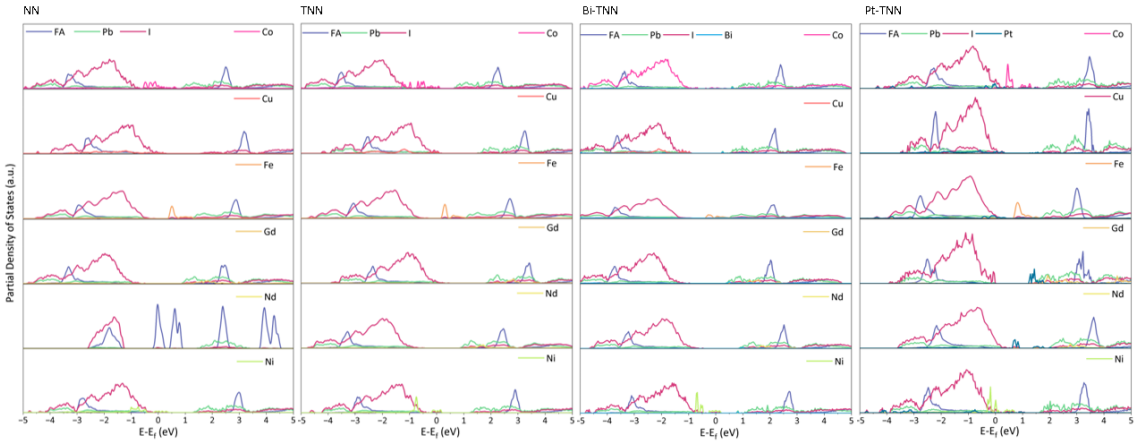

Figure 3.4 PDOS for NN, TNN, Bi-TNN, and Pt-TNN configurations. The graphs illustrate the projected electronic states of both the dopants and the host $FAPbI_3$ lattice, highlighting the influence of doping on the electronic structure, particularly the shifts in the DOS and their impact on material stability.

material. Such stabilization effects highlight the role of the dopant in minimizing lattice distortions and enhancing the overall stability of the structure.

Among the dopants, Gd stands out, particularly in the TNN configurations, due to its ability to maintain a well-defined band structure with minimal defect states and reduced band leakage. This behavior underscores Gd's significant potential in stabilizing the electronic structure and improving the overall performance of the material, making it a promising candidate for enhancing the stability of hybrid perovskites in various applications. This demonstrates that Gd dopants preserve the electronic uniformity of the lattice and stabilize the structure through strong bonding interactions. This observation is further supported by the absence of mid-gap states, which often function as charge traps and negatively impact the material's performance. This finding underscores Gd's potential to improve the optoelectronic and magnetic properties of the material, positioning it as a promising dopant for the development of hybrid perovskites with enhanced functionality for spintronic and energy storage applications.

In conclusion, the analysis of PDOS reveals significant trends in the electronic structure of $FAPbI_3$ doped with various transition metals and rare-earth elements. Cu plays a key role in maintaining the structural and electronic integrity of the

lattice in NN configurations, while Gd demonstrates a strong ability to preserve the lattice's electronic uniformity in TNN configurations. These insights highlight the critical role of dopant selection in stabilizing the material's electronic properties, with the potential to significantly enhance the performance of hybrid perovskites. Further research focusing on the optimization of dopant concentrations and the exploration of additional dopants could pave the way for the development of highly efficient, multifunctional materials for next-generation optoelectronic and spintronic devices.

4. CONCLUSION

This study systematically examined the structural, electronic, and magnetic responses of hybrid perovskite structures under various doping scenarios. The effects of different dopant elements were evaluated, and among them, Gd- and Cu-doped configurations were found to exhibit particularly favorable magnetic characteristics. First-principles calculations revealed that, in certain configurations, these dopants enhance structural stability and induce notable magnetization through spin polarization.

Electronic band structure and density of states analyses indicated that the doped structures retain their semiconducting nature while also acquiring magnetic properties that may be suitable for spintronic applications. These findings suggest that the type, location, and interaction distance of the dopant play a critical role in designing materials with desired magnetic behaviors.

In conclusion, this work demonstrates that doped hybrid perovskite structures hold promise not only for traditional photovoltaic purposes but also for emerging applications in magnetic semiconductors and spintronic technologies. The presented results contribute to the growing body of research focused on tailoring functional materials, providing a solid foundation for future advancements in next-generation spintronic and energy storage systems. Further investigations involving different

dopant types, concentrations, and configurations are likely to deepen understanding and enhance the performance potential of these materials.

REFERENCES

[1] S. M. Yakout, "Spintronics: Future technology for new data storage and communication devices," *Journal of Superconductivity and Novel Magnetism*, vol. 33, 09 2020.

[2] A. Hirohata, K. Yamada, Y. Nakatani, I.-L. Prejbeanu, B. Diény, P. Pirro, and B. Hillebrands, "Review on spintronics: Principles and device applications," *Journal of Magnetism and Magnetic Materials*, vol. 509, p. 166711, 2020.

[3] K. Burke and L. O. Wagner, "Dft in a nutshell," *International Journal of Quantum Chemistry*, vol. 113, no. 2, pp. 96–101, 2013.

[4] International Energy Agency, "Clean energy market monitor – march 2024," 2024. Licence: CC BY 4.0, Accessed:19-May-2024.

[5] J. Wood, "The world added 50% more renewable capacity last year than in 2022," 2024. Accessed: 19-May-2024.

[6] International Renewable Energy Agency, "World energy transitions outlook 2023," 2023. Accessed: 18-May-2024.

[7] Z. Chen, C. Wang, J. Xue, J. Chen, L. Mao, H. Liu, and H. Lu, "Observation of ferromagnetism in dilute magnetic halide perovskite semiconductors," *Nano Letters*, vol. 24, no. 10, pp. 3125–3132, 2024.

[8] Q. Xu, A. Stroppa, J. Lv, X. Zhao, D. Yang, K. Biswas, and L. Zhang, "Impact of organic molecule rotation on the optoelectronic properties of hybrid halide perovskites," *Phys. Rev. Mater.*, vol. 3, p. 125401, Dec 2019.

[9] I. Bergenti and V. Dediu, "Spinterface: A new platform for spintronics," *Nano Materials Science*, vol. 1, no. 3, pp. 149–155, 2019.

[10] S. Wang, W. Xiao, and F. Wang, "Structural, electronic, and optical properties of cubic formamidinium lead iodide perovskite: a first-principles investigation," *Royal Society of Chemistry*, vol. 10, pp. 32364–32369, 01 2020.

[11] P. Canca López, "Study and design of new photovoltaic materials through ab-initio methods.." Unpublished, 2021.

[12] P. Hohenberg and W. Kohn, "Inhomogeneous electron gas," *Phys. Rev.*, vol. 136, pp. B864–B871, Nov 1964.

[13] W. Kohn and L. J. Sham, "Self-consistent equations including exchange and correlation effects," *American Institute of Physics*, vol. 140, pp. A1133–A1138, 11 1965.

[14] H. Xue, *Defects in Halide Perovskites from First Principles*. Phd thesis 1 (research tu/e / graduation tu/e), Applied Physics and Science Education, Dec. 2022. Proefschrift. - Embargo. - pdf open access 21-6-2023.

[15] N. Hernández-Haro, J. Ortega-Castro, Y. Martynov, R. G. Nazmitdinov, and A. Frontera, "Dft prediction of band gap in organic-inorganic metal halide perovskites: An exchange-correlation functional benchmark study," *Elsevier BV*, vol. 516, pp. 225–231, 01 2019.

[16] J. P. Perdew, K. Burke, and M. Ernzerhof, "Generalized gradient approximation made simple," *American Physical Society*, vol. 77, pp. 3865–3868, 10 1996.

[17] J. Tao, J. P. Perdew, V. N. Staroverov, and G. E. Scuseria, "Climbing the density functional ladder: Nonempirical meta–generalized gradient approximation designed for molecules and solids," *American Physical Society*, vol. 91, 09 2003.

[18] J. P. Perdew, K. Burke, and M. Ernzerhof, "Generalized gradient approximation made simple," *American Physical Society*, vol. 77, pp. 3865–3868, 10 1996.

[19] Y. Wang, C. Song, J. Zhang, and F. Pan, "Spintronic materials and devices based on antiferromagnetic metals," *Progress in Natural Science: Materials International*, vol. 27, no. 2, pp. 208–216, 2017.

[20] P. Hohenberg and W. Kohn, "Inhomogeneous electron gas," *Phys. Rev.*, vol. 136, pp. B864–B871, Nov 1964.

[21] R. M. Martin, *Electronic Structure: Basic Theory and Practical Methods*. Cambridge University Press, 2 ed., 2020.

[22] W. Kohn and L. J. Sham, "Self-consistent equations including exchange and correlation effects," *Phys. Rev.*, vol. 140, pp. A1133–A1138, Nov 1965.

[23] E. Mosconi, A. Amat, M. Nazeeruddin, M. Graetzel, and F. Angelis, "First-principles modeling of mixed halide organometal perovskites for photovoltaic applications," *The Journal of Physical Chemistry C*, vol. 117, p. 13902–13913, 07 2013.

[24] W.-J. Yin, T. Shi, and Y. Yan, "Unique properties of halide perovskites as possible origins of the superior solar cell performance," *Advanced materials (Deerfield Beach, Fla.)*, vol. 26, 07 2014.

[25] S.-H. Wei and A. Zunger, "Role of metal d states in ii-vi semiconductors," *Physical review. B, Condensed matter*, vol. 37, pp. 8958–8981, 06 1988.

[26] G. Kresse and J. Furthmüller, "Efficiency of ab-initio total energy calculations for metals and semiconductors using a plane-wave basis set," *Elsevier BV*, vol. 6, pp. 15–50, 07 1996.

[27] M. Fu, P. Tamarat, j.-b. Trebbia, M. Bodnarchuk, M. Kovalenko, J. Even, and B. Lounis, "Unraveling exciton–phonon coupling in individual fapbi3 nanocrystals emitting near-infrared single photons," *Nature Communications*, vol. 9, p. 3318, 08 2018.

[28] I. Žutić, J. Fabian, and S. Das Sarma, "Spintronics: Fundamentals and applications," *Rev. Mod. Phys.*, vol. 76, pp. 323–410, Apr 2004.

[29] P. Cantini, G. Boato, and R. Colella, "Surface charge density waves observed by atomic beam diffraction," *Physica B+C*, vol. 99, no. 1, pp. 59–63, 1980.

[30] W.-J. Yin, T. Shi, and Y. Yan, "Unusual defect physics in ch3nh3pbi3 perovskite solar cell absorber," *Applied Physics Letters*, vol. 104, pp. 063903–063903, 02 2014.

[31] E. Mosconi, A. Amat, M. Nazeeruddin, M. Graetzel, and F. Angelis, "First-principles modeling of mixed halide organometal perovskites for photovoltaic applications," *The Journal of Physical Chemistry C*, vol. 117, p. 13902–13913, 07 2013.

[32] I. Žutić, J. Fabian, and S. Das Sarma, "Spintronics: Fundamentals and applications," *Rev. Mod. Phys.*, vol. 76, pp. 323–410, Apr 2004.

[33] N. Nagaosa, J. Sinova, S. Onoda, A. H. MacDonald, and N. P. Ong, "Anomalous hall effect," *Rev. Mod. Phys.*, vol. 82, pp. 1539–1592, May 2010.

[34] K. Momma and F. Izumi, "*VESTA3* for three-dimensional visualization of crystal, volumetric and morphology data," *Journal of Applied Crystallography*, vol. 44, pp. 1272–1276, Dec 2011.

[35] G. Kresse and J. Häfner, "Ab initio molecular dynamics for liquid metals," *American Physical Society*, vol. 47, pp. 558–561, 01 1993.

[36] V. Wang, N. Xu, J.-C. Liu, G. Tang, and W.-T. Geng, "Vaspkit: A user-friendly interface facilitating high-throughput computing and analysis using vasp code," *Computer Physics Communications*, vol. 267, p. 108033, 05 2021.